Soil respiration in perennial grass and shrub ecosystems: Linking environmental controls with plant and microbial sources on seasonal and diel timescales

Mariah S. Carbone,[1,2] Gregory C. Winston,[1] and Susan E. Trumbore[1]

Received 28 September 2007; revised 14 January 2008; accepted 1 February 2008; published 13 May 2008.

[1] A mechanistic understanding of soil respiration is a major impediment to predicting terrestrial C fluxes spatially and temporally. Automated measurements of soil respiration offer the high-resolution information necessary to observe temporal variation in soil respiration, but spatially these measurements are under-represented in water-limited and non-forested ecosystems. We measured soil respiration with automated chambers over the growing season, at two sites with the same semi-arid climate, but with different dominant vegetation, perennial grasses and shrubs in the Owens Valley, CA, USA. An isotope mass balance technique was used to partition soil respiration into autotrophic and heterotrophic components at two time points, early and late growing season. Results showed large differences in the magnitude of growing season soil respiration between the two sites (910 versus 126 g C m^{-2} for grasses and shrubs respectively over 5 months). We attribute this to site differences in soil water availability and belowground allocation and productivity. Diel patterns of soil respiration between the two sites were similar. Temperature explained most of the diel variability in the early growing season, when soil moisture was greatest. As soil moisture declined over the growing season, diel patterns became increasingly decoupled temporally from temperature due to increased water-limitation on surface heterotrophic sources and hypothesized strong photosynthetic control over soil respiration rates. Partitioning of soil respiration into autotrophic and heterotrophic sources showed the dominance of autotrophic sources across seasons and ecosystems. However, heterotrophic respiration was more dynamic from early to late growing season, declining in the grass ecosystem; and a surprising increase in the shrub ecosystem, attributed to warming of the soil profile enhancing microbial decomposition at depth.

Citation: Carbone, M. S., G. C. Winston, and S. E. Trumbore (2008), Soil respiration in perennial grass and shrub ecosystems: Linking environmental controls with plant and microbial sources on seasonal and diel timescales, *J. Geophys. Res.*, *113*, G02022, doi:10.1029/2007JG000611.

1. Introduction

[2] Soil respiration is one of the largest and most variable fluxes of CO_2 to the atmosphere, and potentially sensitive to future changes in climate [*Cox et al.*, 2000; *Raich et al.*, 2002]. Major driving variables used to model soil respiration include temperature, water content, and substrate supply [*Davidson et al.*, 2006]. Yet, predicting soil respiration with models continues to be challenging because it integrates two very different processes that are methodologically difficult to separate: root respiration (autotrophic respiration) and microbial decomposition of soil organic matter (heterotrophic respiration) [*Hanson et al.*, 2000]. Hence how variables like temperature influence the different sources of soil respiration in space and time remains a major gap in our present understanding of the global C cycle.

[3] Over monthly and annual timescales, soil respiration rates have been related to temperature, soil moisture, and productivity [*Raich and Schlesinger*, 1992; *Raich and Potter*, 1995; *Davidson et al.*, 1998; *Janssens et al.*, 2001; *Reichstein et al.*, 2003]. On the diel timescale, temperature, moisture pulses, and photosynthesis rates have been shown to be important drivers of soil respiration across a range of ecosystem types [*Craine et al.*, 1999; *Högberg et al.*, 2001; *Kuzyakov and Cheng*, 2001; *Huxman et al.*, 2004; *Xu et al.*, 2004; *Tang et al.*, 2005; *Baldocchi et al.*, 2006; *Liu et al.*, 2006]. Over both timescales, soil respiration is still largely described with empirical models based on site-specific relationships [*Davidson et al.*, 2006]. Accurately modeling soil respiration on a per-site basis provides valuable information for gap filling and partitioning of net ecosystem exchange to ecosystem respiration and gross ecosystem exchange [*Richardson et al.*, 2006]. However, ultimately these simple empirical relationships do not offer the predic-

[1] Department of Earth System Science, University of California, Irvine, California, USA.
[2] Now at Department of Geography, University of California, Santa Barbara, California, USA.

0148-0227/08/2007JG000611

tive capability necessary to upscale fluxes to the regional or global level.

[4] In order to advance the understanding of soil respiration (i.e., develop models based on mechanistic relationships) we must identify how environmental variables affect the individual sources of soil respiration spatially and temporally [*Davidson et al.*, 2006; *Trumbore*, 2006]. The more recent availability of high-time resolution automated measurements of soil respiration has provided the detailed information necessary to explain temporal variation in fluxes [*Irvine and Law*, 2002; *Savage and Davidson*, 2003; *Tang and Baldocchi*, 2005; *Carbone and Vargas*, 2008]. However, these automated soil respiration studies (and most manual studies) have been spatially limited to a few ecosystem types, most of which conducted in mesic and/or forested ecosystems [*Raich and Schlesinger*, 1992; *Goulden and Crill*, 1997; *Irvine and Law*, 2002; *King and Harrison*, 2002; *Savage and Davidson*, 2003; *Reichstein et al.*, 2002; *Liu et al.*, 2006; *Tang et al.*, 2005]. Moreover, soil respiration measurements in water-limited (i.e., semi-arid and arid) ecosystems are generally under-represented in reviews and synthesis studies [*Raich and Potter*, 1995; *Subke et al.*, 2006]. Expanding the breadth of ecosystems examined with high-resolution soil respiration measurements will provide new information about relationships between environmental variables, vegetation types and soil respiration rates. For example, in most mesic ecosystems temperature and precipitation often co-vary with confounding phenological changes [*Davidson et al.*, 1998], but in many semi-arid and arid ecosystems temperature, precipitation and phenology may have different temporal relationships [*Reichstein et al.*, 2002; *Tang and Baldocchi*, 2005].

[5] In terms of the global C budget, semi-arid and arid regions are of further interest because many have undergone vegetation shifts from herbaceous to woody species [*Schlesinger et al.*, 1990; *Jackson et al.*, 2000; *Asner et al.*, 2003; *Elmore et al.*, 2003]. Shifts in dominant plant types from grasses to shrubs (due to many, primarily human causes) can increase standing biomass, alter root and leaf litter inputs, change spatial distributions of organic matter and nutrients, and alter soil C storage [*Jackson et al.*, 2000]. Thus understanding vegetation type controls on soil respiration rates, like allocation patterns and phenology, are also important for future predictions of atmospheric CO_2. Surprisingly, there are few studies of continuous soil respiration measurements in these dry environments, and to our knowledge, none that directly compare co-occurring perennial grass and shrub ecosystems.

[6] Consequently, this study was initiated to examine basic patterns and sources of soil respiration in perennial grass and shrub ecosystems in the Owens Valley, CA, USA. In this paper, we present simple empirical models on seasonal and diel timescales to demonstrate soil respiration temperature and moisture relationships over the growing season, and for comparison to previous soil respiration work. However, our research goal was to take the analyses beyond this basic understanding by combining high-resolution measurements of soil respiration with isotope (radiocarbon) source partitioning techniques. We had specific interest in: (1) quantifying and separating autotrophic and heterotrophic sources of soil respiration, (2) determining the environmental controls on soil respiration over seasonal and diel timescales, and (3) linking how these controls and sources interact in time to resolve soil respiration patterns in the perennial grass and shrub ecosystems.

2. Site Description

[7] This study was conducted over two growing seasons in 2005–2006 in the Owens Valley, California, USA, near the city of Bishop (37°60′N, 118°60′W). The Owens Valley is located in eastern California, in the rain shadow of the Sierra Nevada Mountains at ~1250 m elevation. The climate is like that of the nearby Great Basin desert, with average temperatures ranging from 11/6°C (daytime high/nighttime low) in winter to 37/14°C in summer. Average annual precipitation is ~150 mm, 75% of which falls in the winter months between November and March, when plants are dormant. However, in the spring and summer, runoff from the snowpack in the Sierra Nevada and White-Inyo Mountains flows into the valley resulting in a high groundwater table [*Hollett et al.*, 1991], providing an additional water supply for the vegetation on the valley floor.

[8] Two sites were selected that differed in dominant vegetation typical of the Great Basin desert. The grass site was an alkali meadow plant community, dominated by the C_4 perennial grasses *Distichlis spicata* (inland saltgrass) and *Juncus balticus* (wirerush). The shrub site was a phreatophytic scrub plant community dominated by the winter deciduous C_3 perennial shrubs *Ericameria nauseosa* (rubber rabbitbrush, formerly *Chrysothamnus naseosus)* and *Sarcobatus vermiculatus* (greasewood). Both plant types had similar phenology, and were phreatophytic (groundwater using plants). New growth began in the spring (April), the maximum leaf area was reached by early summer (June), and flowering occurred in middle to late summer (late June–August). The grasses lost contact with the groundwater in late summer resulting in earlier senescence than the shrubs, which were deeper-rooted and maintained access to groundwater throughout the growing season [*Pataki et al.*, 2008]. Additional background site characteristics are described in Table 1.

3. Methods

3.1. Automated Measurements of Soil Respiration

[9] Two automated soil respiration measurement systems were developed and built at UC Irvine, based on the design of *Goulden and Crill* [1997]. Each consisted of eight dark chambers, constructed of white PVC sewer pipe (25 cm ID, 21 cm tall, ~11 l volume) with a thermistor (EC95H303W, Thermometrics, Edison, NJ, USA) in each chamber top to measure air temperature. Chamber tops were automatically lowered and raised from the soil surface by pneumatic air cylinders, and sealed to chamber bottoms by silicon tubing o-rings. The two systems differed in how the chamber bottoms were sealed to the soil surface. The system used at the shrub site had a shallow collar that was inserted 3–4 cm into the sandy soil surface. The second system operated at the grass site used a sand-ring diffusion barrier to seal to the soil surface; these chamber collars did not penetrate the soil. Both systems were independently tested

Table 1. Site Characteristics

	Grass Site	Shrub Site
Location	37° 24.71′N 118° 25.59′W	37° 19.30′N 118° 21.50′W
Dominant vegetation	*Distichlis spicata*, *Juncus balticus*	*Ericameria nauseosa*, *Sarcobatus vermiculatus*
Max leaf area index, $m^2\ m^{-2}$	1.0–1.7	0.3–1.1
Depth to water table, m	1–2	1.7–>2.5
Soil clay/silt/sand fractions, %	13.0/47.7/39.3	3.5/17.5/79.0
Soil pH	8.5	9.1
Soil salinity, ds m^{-1}	16.0	0.9
Soil carbon content, %	6.1	0.52
Soil nitrogen content, %	0.4	0.04
Soil C stocks, kg C m^{-2}	24.81	0.90

in the laboratory and field for leaks with CO_2 standard additions. At the grass site, live aboveground biomass was removed in from the chambers by clipping at the soil surface. Adjacent grass roots extended underneath all chambers, and were assumed to be representative of soil respiration. At the shrub site, the chambers were evenly distributed near plants and in interspaces to best capture natural spatial variability; fine root growth was observed months after the collars were inserted. No aboveground portions of living plants were in the chambers at either site.

[10] Both systems were completely solar powered, and had identical control boxes and air compressors that operated the chambers. The control box consisted of a CR10X data logger (Campbell Scientific, Logan, UT, USA) controlling a Campbell SM16 storage module, LI-840 infrared gas analyzer (IRGA; Li-Cor, Lincoln, NE, USA), 2 Campbell SDM-CD16AC relay controllers, 3 solenoid valve manifolds, a pump, flowmeter, and a needle valve flow controller. The CO_2 concentration and air temperature within each chamber was logged every 20 s for a total of 12 min. The first 2 min with the chamber top open to flush the tubing with ambient air, and for the remaining 10 min after the chamber top had sealed to the chamber bottom. The air from the chamber was circulated to the IRGA and back to the chamber at $\sim$1 l min^{-1}. To calculate soil respiration rates, the change in CO_2 concentration with time (after the first 2 min of measurements, which recorded ambient air only) was fitted to a 2nd order polynomial equation using a least squares regression. The value of the 1st derivative of the fitted equation at the point where the equation was equal to ambient CO_2 concentrations (dC/dt) was used to calculate soil respiration with the following equation:

$$R_S = dC/dt \times \left(V_{sys}/A_b\right) \times \left(P_{atm}/(R \times T_{ch})\right) \quad (1)$$

where, R_S is soil respiration (reported here in mg C m^{-2} h^{-1}), V_{sys} is the volume of the system (i.e., chamber headspace plus tubing), A_b is the basal area covered by the chamber, P_{atm} is the atmospheric pressure, R is the gas constant, and T_{ch} is the temperature of the air inside the chamber. V_{sys} for each chamber was determined, and the whole system was leak-checked, 4 times over the course of measurements by standard addition of a CO_2 reference gas.

[11] At the same frequency as the soil respiration measurements, additional environmental information was collected on a meteorological station at each site. These included air (Campbell CS105) and litter (HMP44L; Vaisala Oyj, Vantaa, Finland) temperature and relative humidity; soil temperature at 2 cm, 20 cm and 35 cm (Thermometrics EC95H303W); volumetric water content (VWC) at 20 and 35 cm depths (Campbell CS616); fuel moisture at the soil surface (Campbell CS505); atmospheric pressure (Campbell C115); photosynthetically active radiation (PAR; LiCor LI-190); and wind speed and direction (Campbell RM3101 and RM3301). Soil moisture data were calibrated using measurements of gravimetric water content and soil bulk density (A. Steinwand, personal communication). Soil matric potential was calculated using soil sand and clay fractions following *Saxton et al.* [1986]. Vapor pressure deficit (VPD) was calculated using air temperature and relative humidity measurements.

[12] The soil profile pore space CO_2 concentration was determined by vertically inserting 0.9 cm ID stainless steel tubes into the ground to depths of 5, 10, 25, 50, and 100 cm. The tubes were open and perforated for 5 cm at the bottom, and sealed at the top (aboveground) with a gas tight fitting and a septa for sampling. Four sets of tubes of each depth class were installed within the area of the automated chamber measurements. The CO_2 concentration was measured by removing two tube volumes, then filling a 60 mL syringe with soil air and injecting into an LI-840 IRGA with a 2 cm cell (measures concentrations to 2% CO_2).

3.2. Soil Respiration Analyses and Modeling

[13] The soil respiration data were separated into 8 representative 3-day time periods that were distributed evenly over the growing season ($\sim$every 20 days), but excluded times immediately following small rain events, and those with data gaps. These 8 data sets were used to model soil respiration on a diel timescale, and the means of each time period were collectively used to model soil respiration over the growing season. All soil respiration data sets were first fit to a temperature model using a non-linear least squares regression. The residuals of the temperature model were then fit to a soil moisture model like that described by *Savage and Davidson* [2003]. The equation used for temperature was:

$$R_S = A \times e^{B \times T} \quad (2)$$

Where T is temperature (with best fit, either air or 2 cm soil temperature) and A and B are the fitted parameters of the model. The temperature sensitivity of soil respiration was assessed using the Q_{10} value, defined as the change in soil

respiration for a given 10°C increase in temperature, calculated by:

$$Q_{10} = e^{B\times 10} \quad (3)$$

The soil moisture model was either linear (for diel models) or parabolic (for seasonal models).

$$r_T = a \times VWC + b \quad (4)$$

or

$$r_T = a^2 \times VWC + b \times VWC + c \quad (5)$$

Where r_T is the residual of the temperature model, VWC is the volumetric soil water content, and a, b and c are the fitted parameters of the model. The final soil respiration models took the form:

$$R_S = A \times e^{(B\times T)} + a \times VWC + b \quad (6)$$

or

$$R_S = A \times e^{(B\times T)} + a^2 \times VWC + b \times VWC + c \quad (7)$$

3.3. Soil Respiration Isotopic Measurements

[14] Isotopic measurements of the ^{14}C content in soil respiration were made automatically with a trapping system attached to the automated chamber system. Samples were collected at two time points of the study; during the early growing season and during the late growing season (DOY 120–122 and 201–203, corresponding to time periods 2 and 6). During the final 2 min of each chamber measurement, the accumulated CO_2 was collected by diverting the airflow through a $MgClO_4$ drying column via a manifold to an activated molecular sieve 13 × trap that quantitatively removed CO_2 [*Gaudinski et al.*, 2000]. The remaining air was then returned to the chamber as before. An ambient air $^{14}CO_2$ sample was also collected in the same manner by diverting air from an open chamber. Samples were collected over 3, 96 min measurement cycles of the entire chamber system between the hours of 8:00 and 14:00.

3.4. Isotopic Measurements of End-Members

[15] Field incubations were used to determine the ^{14}C signature of root respiration (autotrophic respiration, $\Delta^{14}C_A$) following *Czimczik et al.* [2006]. Fine roots (<2 mm; but excluding extremely fine <0.2 mm roots) were collected from soil blocks 20 × 20 cm square, and 10–15 cm deep that were excavated from 4 locations at each site. Roots were extracted from the soil by hand, rinsed with water and placed in an air tight 2 l incubation jar with gas in- and outlets on the lid. The jars were flushed with CO_2 free air and placed in a dark ice chest to maintain temperatures close to in situ conditions. The CO_2 was allowed to accumulate to at least 1000 ppm (~2 h). The CO_2 concentration was measured with an IRGA, and collected by passing incubation air through a $MgClO_4$ drying column to a molecular sieve trap. It was not possible to sample surface roots for incubation in the late growing season, due to very dry surface soil conditions. Average atmospheric air ^{14}C signatures were used instead because a concurrent pulse-labeling study at these sites [*Carbone and Trumbore*, 2007] demonstrated that root respiration was overwhelmingly derived from current-year photosynthetic products.

[16] Laboratory incubations of soil organic matter (SOM) were used to determine the ^{14}C signature from microbial decomposition (heterotrophic respiration, $\Delta^{14}C_H$) following *Schuur and Trumbore* [2006]. A soil pit was excavated at each site in May, 2006 to approximately 65 cm depth. Soil samples were collected to represent surface (upper 20 cm) and deep (50–65 cm) SOM, refrigerated immediately and returned to UC Irvine for laboratory incubations. The fine roots were left intact and were presumed to have died during this time interval, while coarse roots (>2 mm) were gently removed. Soils were placed in l l incubation jars with gas tight lids, and flushed with CO_2 free air. From each site, 2–3 replicates of SOM were incubated at room temperature. The CO_2 concentration in each jar was measured daily using an IRGA to monitor the rate of CO_2 production and to ensure CO_2 concentrations did not exceed soil gas CO_2 values observed in the field. After 7 days (enough time for fine roots to cease respiration), the jars were flushed with CO_2 free air, and left to accumulate CO_2 for ~2–5 days depending on the production rate. For ^{14}C analyses, the accumulated CO_2 was collected from the jar head-space with an evacuated 0.5 l flask.

3.5. Radiocarbon Analyses

[17] All CO_2 samples were extracted from the molecular sieve or flask, purified on a vacuum line, and converted to graphite [*Xu et al.*, 2007]. The ^{14}C content of the graphite was measured using accelerator mass spectrometry (NEC 0.5MV 1.5SDH-2 AMS system) at the W. M. Keck-CCAMS facility of UC Irvine [*Southon et al.*, 2004]. The radiocarbon data ($\Delta^{14}C$) are reported in per mil (‰), the deviation (in parts per thousand) of the ratio of $^{14}C/^{12}C$ in a sample divided by that of a standard of fixed isotopic composition (0.95 times the $^{14}C/^{12}C$ of oxalic acid I standard, decay corrected to 1950). As reported, measurements have been corrected for the effects of mass-dependent isotope fractionation by normalizing to a common $\delta^{13}C$ value (−25‰) and assuming ^{14}C is fractionated twice as much as ^{13}C [*Stuiver and Polach*, 1977]. For this purpose, the $^{13}C/^{12}C$ of each sample was concurrently measured by AMS. High precision $\delta^{13}C$ of each sample was determined on Thermo Electron Gas Bench II coupled with a Delta Plus IRMS by taking aliquots of CO_2 prior to graphitization.

[18] Radiocarbon values from the soil respiration chamber measurements were first corrected for the atmospheric CO_2 that was already present in the chamber when the top was closed, because chambers were not flushed with CO_2 free air before collection. This was done using the following isotope mixing model:

$$\Delta^{14}C_{Rs} = \left(\left(\Delta^{14}C_M \times [CO_2]_M\right) - \left(\Delta^{14}C_{AIR} \times [CO_2]_{AIR}\right)\right)/[CO_2]_{Rs} \quad (8)$$

where $\Delta^{14}C_M$, $\Delta^{14}C_{AIR}$, $\Delta^{14}C_{Rs}$ are the signatures of the measured sample, air, and soil respiration respectively, and $[CO_2]_M$, $[CO_2]_{AIR}$, $[CO_2]_{Rs}$ are the CO_2 concentrations of

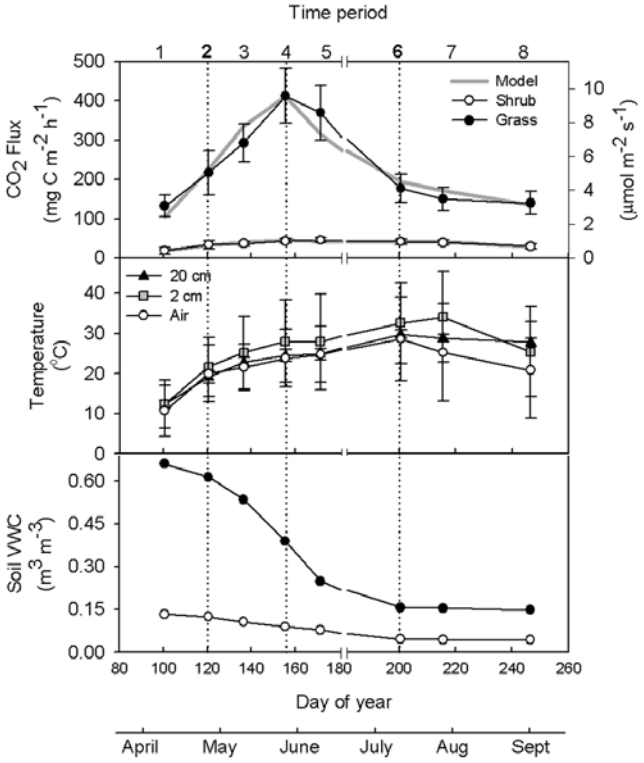

Figure 1. Mean of continuous measurements from defined diel time periods 1–8, for grass (black circles) and shrub (white circles) soil respiration, seasonal models (grey lines) air temperature (white circles), 2 cm (grey squares) and 20 cm (black triangles) soil temperature, and volumetric water content at 20 cm depth. Dotted lines indicate time periods where the mean diel cycles are shown in Figure 4, and also include those where soil respiration source partitioning took place (periods 2 and 6; shown in Figure 5). Break separates 2006 (before) from 2005 (after) growing season. Error bars represent ±1 standard deviation, and are sometimes smaller than the size of the symbol.

the measured sample, air, and soil respiration, respectively, in the field at the time of sampling.

3.6. Partitioning the Sources of Soil Respiration

[19] The radiocarbon signatures were used to partition soil respiration ($\Delta^{14}C_{Rs}$) by means of an isotope mass balance approach, with the end-members for autotrophic ($\Delta^{14}C_A$) and heterotrophic ($\Delta^{14}C_H$) respiration determined by the incubations of roots and SOM, respectively. The single isotope two source mixing model and error propagation methods from *Phillips and Gregg* [2001] was applied. Surface SOM incubation signatures were used to represent heterotrophic respiration in the early growing season at both sites, and also at the grass site in the late growing season. Because of extreme desiccation stress in surface soil in the shrub ecosystem (<−1500 kPa matric potential), the deep SOM incubation signature was used to represent heterotrophic respiration in the late growing season.

[20] There are notable biases to partitioning soil respiration with this technique [*Gaudinski et al.*, 2000]. While isotopes offer the advantage of partitioning soil respiration in situ with less disturbance in comparison to other methods such as girdling and trenching [*Hanson et al.*, 2000], in making our measurements we assumed that autotrophic sources would be fast cycling (short ecosystem residence times) and that our incubations would accurately integrate the contributions of faster and slower cycling heterotrophic sources (resulting in overall longer ecosystem residence times). The microbial use of fast cycling C (i.e., mycorrhizal respiration and the decomposition of root exudates) will produce a ^{14}C signature like that of an autotrophic source, but in fact should contribute to our incubation measurement of total heterotrophic respiration. However, rapid decomposition of these rhizosphere components in the time interval between sampling and the start of our incubations would mean that this component is under-represented in our heterotrophic end-member ^{14}C signature. Hence the most likely bias in our results is an underestimate of the fast-cycling heterotrophic component, which would lead to an overestimate of autotrophic respiration sources.

[21] Soils at these sites contained highly variable amounts of calcium carbonate, which we determined had mean signatures for $\delta^{13}C$ of −2.9‰ and $\Delta^{14}C$ of −32‰. By keeping CO_2 concentrations within the incubation jars close to those found in soil CO_2, we minimized the possibility of CO_2 derived from acidification of these carbonates to our incubation sample CO_2. The lack of heavy stable isotopes and the agreement among replicates (which had differing amounts of carbonate) indicated that carbonates were not a major contributor of CO_2 in our incubations or in the chamber measurements in the field.

4. Results

4.1. Seasonal Patterns in Soil Respiration and Environmental Variables

[22] The seasonal patterns of soil respiration were derived from the daily mean of continuous measurements for diel time periods 1–8 and are shown in Figure 1. Soil respiration rates in the grass ecosystem were much greater than those measured in the shrub ecosystem, almost by an order of magnitude at peak values (412 versus 45 mg C m^{-2} h^{-1}). Rates peaked slightly earlier in the grass than the shrub ecosystem, DOY 158 versus 170, but preceded that of maximum temperature (air and 2 cm soil) in both ecosystems (DOY 200–215). Soil VWC (measured at 20 cm) markedly decreased from DOY 100 to 200 at both sites, remained constant from DOY 200 to 250, but overall absolute and available (soil matric potential, data not shown) soil moisture was much greater in the grass ecosystem than the shrub ecosystem.

[23] Soil respiration rates responded immediately to 3 small precipitation events over the course of the measurements. Precipitation events were not large enough to alter VWC, and only barely wet the surface soil/litter layer, as detected by a surface fuel moisture sensor (data not shown). The magnitude of the response was larger in the shrub ecosystem (as much as 3 times the preceding respiration rate) but the duration of the response was short (less than 2 days) resulting in a negligible contribution to total growing season soil respiration. Cumulative growing season soil respiration (from DOY 100 to 250) was 910 ± 82 and 126 ± 12 g C m^{-2} for the grass and shrub ecosystem respectively.

Table 2. Diel and Seasonal Soil Respiration Model Parameters[a]

Site	Period	DOY	*A*	*B*	Q_{10}	*a*	*b*	*c*	*n*	R^2
Grass	1	100–103	91.7	0.029	1.34				45	0.90
	2	120–123	115.8	0.030	1.35				44	0.77
	3	136–139	174.0	0.024	1.28				44	0.82
	4	154–157	248.4	0.021	1.23				45	0.79
	5	169–172	212.6	0.022	1.25				40	0.79
	6	199–202	126.2	0.011	1.12	19699	−3090		44	0.50
	7	212–215	104.8	0.013	1.14	5558	−856		44	0.66
	8	246	95.0	0.009	1.10				16	0.60
	Season	100–246	135.4	0.022	1.24	−3963	3226	−467	8	0.92
Shrub	1	100–103	5.1	0.087	2.40				45	0.86
	2	120–123	12.8	0.043	1.53				45	0.95
	3	136–139	23.0	0.018	1.20				45	0.82
	4	154–157	30.1	0.013	1.14				45	0.75
	5	169–172	35.9	0.012	1.12				45	0.78
	6	199–202	34.9	0.005	1.05				45	0.52
	7	212–215	29.3	0.008	1.08				45	0.25
	8	246	25.0	−0.001	0.90				16	0.13
	Season	100–246	12.7	0.044	1.55	−5199	933	−35	8	0.92

[a]Diel model form: $R_S = A \times e^{(B \times T)} + a \times VWC + b$. Seasonal model form $R_S = A \times e^{(B \times T)} + a^2 \times VWC + b \times VWC + c$. Where T is temperature (2 cm soil for grass, and air for shrub), and VWC is volumetric water content at 20 cm, and $Q_{10} = e^{B \times 10}$.

[24] Mean growing season soil respiration in the grass ecosystem was 257.9 mg C m^{-2} h^{-1}, and the mean growing season value ranged between 245.6 and 267.5 mg C m^{-2} h^{-1} among individual chambers. At the shrub site, mean growing season soil respiration was 33.5 mg C m^{-2} h^{-1}, and spatial variability was much greater among chambers, in which mean values ranged 23.9 to 47.6 mg C m^{-2} h^{-1}.

4.2. Empirical Models of Soil Respiration

[25] Model parameters (equations (2)–(7)) for the seasonal and diel soil respiration timescales are shown in Table 2. The seasonal soil respiration models are compared with mean soil respiration rates for the 8 identified time periods in Figure 1. The high-resolution measurements showed that the grass soil respiration-temperature relationships had a slightly better fit with 2 cm soil temperature, whereas shrub soil respiration temperature relationships fit best with air temperature (based on r^2 values), and therefore were used for the seasonal models. Both grass and shrub ecosystem seasonal models fit well ($r^2 = 0.92$), and required a parabolic soil moisture relationship. Seasonal basal soil respiration values were 134.7 and 12.7 mg C m^{-2} h^{-1} for the grass and shrub ecosystem respectively. These differed from the time integrated mean of the diel model parameters (149.5 and 25.9 mg C m^{-2} h^{-1}). Seasonal Q_{10} values were 1.24 and 1.55 for the grass and shrub ecosystem respectively, compared to the mean Q_{10} of the diel models (1.22 and 1.24 respectively). Cumulative growing season soil respiration estimates from the fixed parameter seasonal models were 852 ± 68 and 133 ± 11 g C m^{-2} from the grass and shrub ecosystem respectively, within the error of measured values.

[26] Diel soil respiration and diel models for all time periods (excluding period 8) are shown in Figure 2. Most models for the grass and shrub ecosystems fit data well, and

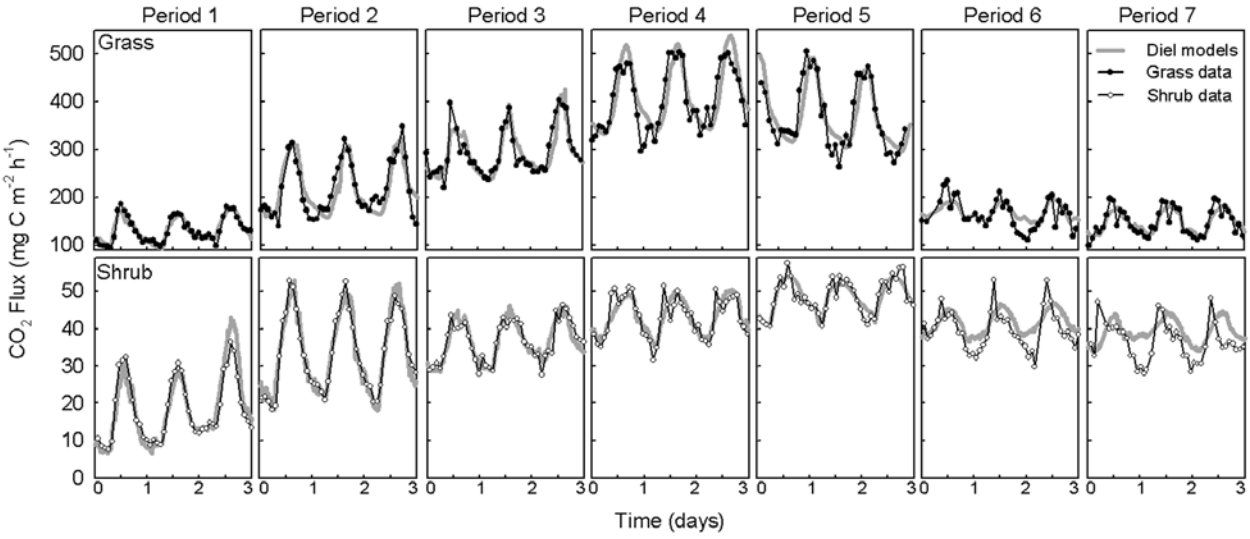

Figure 2. Grass (black circles) and shrub (white circles) soil respiration and diel empirical models (grey line) for time periods 1–7 in both grass and shrub ecosystems.

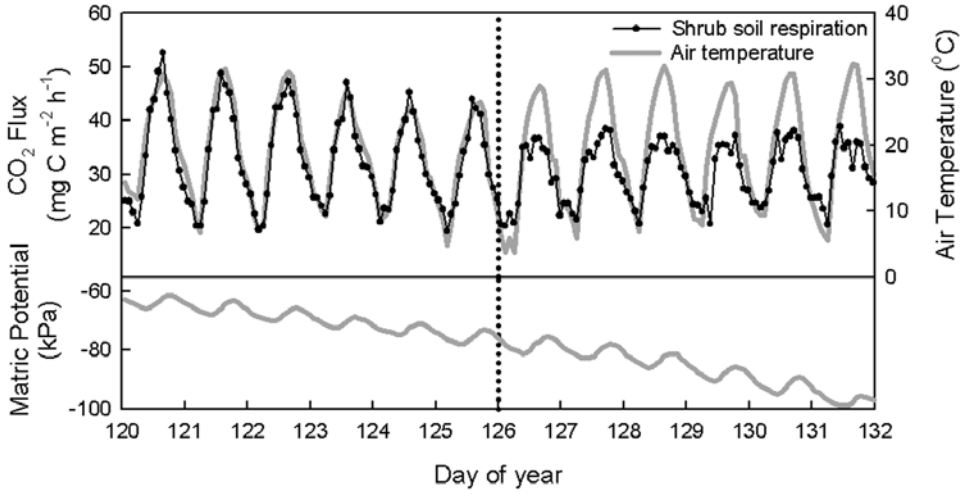

Figure 3. Shrub ecosystem soil respiration (black circles) and air temperature (grey line), and soil water matric potential at 20 cm depth. Dotted line on DOY 126 indicates the onset of a different diel pattern of soil respiration.

required only a temperature relationship to explain the majority of the diel variability (r^2 = 0.75–0.95). Exceptions to this occurred in the middle to late growing season for both ecosystems. The grass periods 6 and 7, required an additional linear soil moisture relationship to explain 30–35 % of the variability (r^2 = 0.50 and 0.66 respectively); and shrub periods 6–8 had weaker temperature relationships, and no soil moisture relationships (r^2 = 0.52, 0.25 and 0.13 respectively). In the grass ecosystem, diel basal soil respiration (parameter A; equation (2)) was lowest in both the early growing and late season (periods 1 and 8, 91.7 and 95.0 mg C m^{-2} h^{-1} respectively) and peaked in period 4 (248.4 mg C m^{-2} h^{-1}). In the shrub ecosystem, basal soil respiration was also at a minimum in the early growing season (period 1, 5.1 mg C m^{-2} h^{-1}), but unlike the grass ecosystem basal soil respiration remained relatively high (period 8, 25.0 mg C m^{-2} h^{-1}) at the end of the measurements. Basal soil respiration in shrubs also peaked later (period 5, 35.9 mg C m^{-2} h^{-1}) than the grasses. Diel temperature sensitivity (Q_{10} values) were greatest in the early growing season (grass = 1.34, shrub = 2.4), and declined (linearly in grass ecosystem, exponentially in shrub) over the course of the growing season to minimum values (grass = 1.10, shrub = 0.90).

4.3. Diel Patterns in Soil Respiration

[27] A very clear change in the diel pattern of shrub soil respiration was observed in the early growing season. Figure 3 shows soil respiration, air temperature and soil matric potential at 20 cm from DOY 120 to 132. From DOY 120 to 126 (and days previous to 120), the diel pattern closely followed that of air temperature. After DOY 126, the diel pattern had smaller amplitude, and became consistently more bimodal in form (also shown in Figure 2, between periods 2 and 3). This pattern did not coincide with abrupt changes in the magnitude of temperature, moisture (matric potential), or any other environmental variable measured. Although, temperature was generally increasing and soil moisture (VWC) and matric potential were decreasing during this time period. A more gradual shift to a bimodal pattern over the growing season occurred in the grass ecosystem roughly between DOY 140–150 (Figure 2, between periods 3 and 4), but it was neither as abrupt nor distinct as observed in the shrub ecosystem.

[28] Looking in greater detail at the diel course of soil respiration, the mean diel cycle for time periods 2 (early May), 4 (mid June), and 6 (late July) are shown in Figures 4a and 4c. In period 2, soil respiration in both grass and shrub ecosystems were in phase with the diel course of temperature. In periods 4 and 6, soil respiration increasingly peaked earlier in the day, before maximum temperature in both ecosystems, and there was noticeable clockwise hysteresis in the temperature-CO_2 flux relationship (Figures 4b and 4d). The bimodal shape of soil respiration (with a small mid-day depression) present in grass periods 4 and 6 and shrub period 4, was consistent across most of the growing season. By period 6, the bimodal shape of the shrub diel cycle lost the second peak, and was unimodal, with peak values skewed toward the morning for the late growing season measurements. From the beginning to the end of the growing season, the diel amplitude had reduced to approximately half original size in both ecosystems. In the grass ecosystem, the amplitude was similar in periods 2 and 4 (150 and 188 mg C m^{-2} h^{-1} respectively), and 81 mg C m^{-2} h^{-1} in period 6. The diel amplitude in the shrub ecosystem was greatest in period 2 (31 mg C m^{-2} h^{-1}) and decreased to 15 and 16 mg C m^{-2} h^{-1} in periods 4 and 6, respectively, where the base respiration rate was almost twice that of period 2. The maximum vapor pressure deficit (VPD) was greatest in the shrub ecosystem, ranging from 3 to larger than 5 kPa, but increased over the growing season in both ecosystems.

4.4. Radiocarbon Signatures of Respired CO_2

[29] Radiocarbon signatures of end-members (root and SOM incubations) and soil respiration are shown in Figure 5. Root respiration $\Delta^{14}C$ values for both the grasses and shrubs fell within the range measured for CO_2 in ambient air at the time of sampling. SOM respiration $\Delta^{14}C$ values were elevated, reflecting the predominance

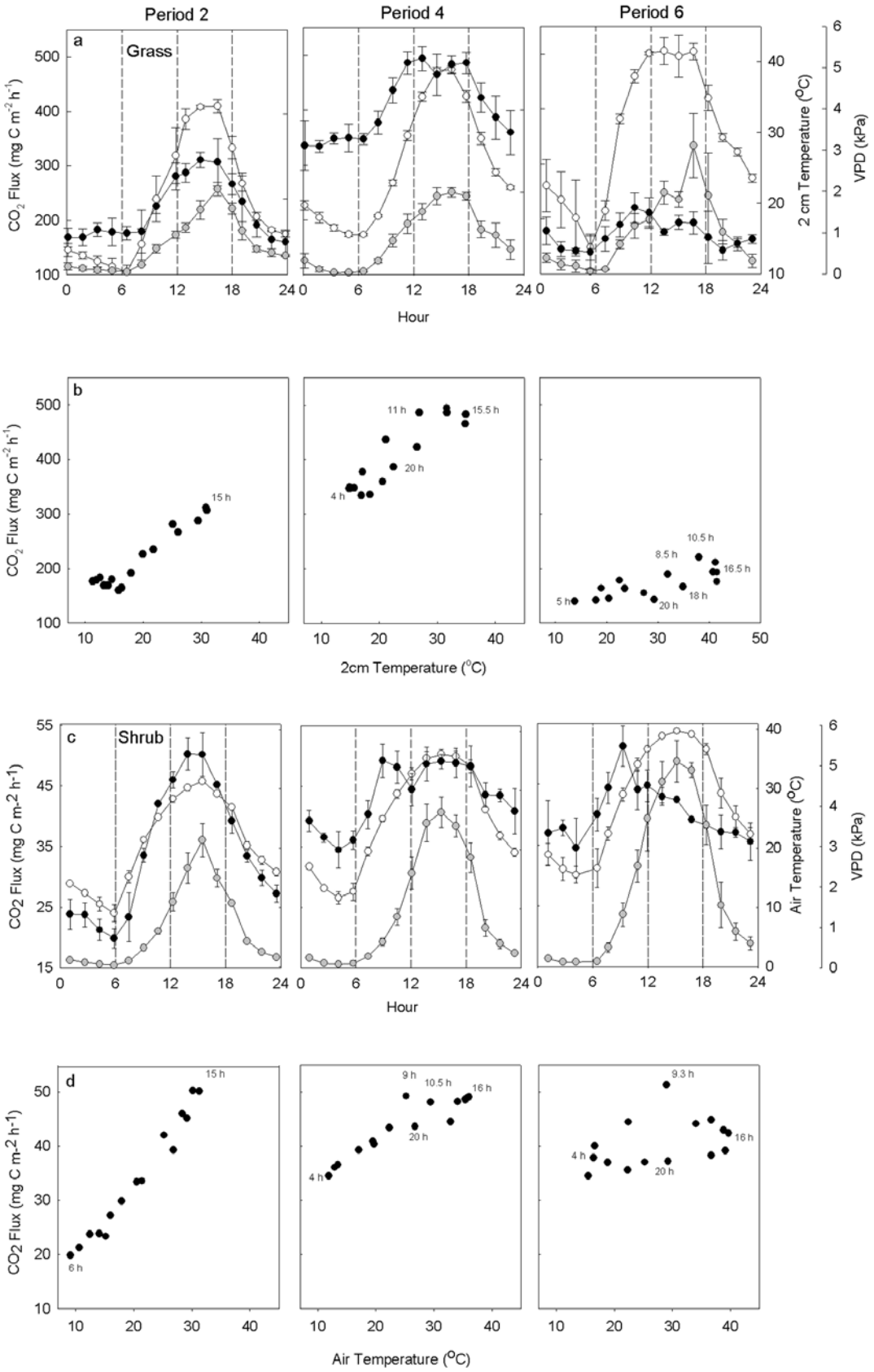

Figure 4. Mean diel cycle of soil respiration (black), temperature (white), and VPD (grey) over time periods 2, 4, and 6 for grass (a) and shrub (c) ecosystems. Mean diel temperature-CO_2 flux relationship for the same time periods in the grass (b) and shrub (d) ecosystems. Numbers in (b) and (d) represent the time of day (hours). Error bars represent ±1 standard deviation.

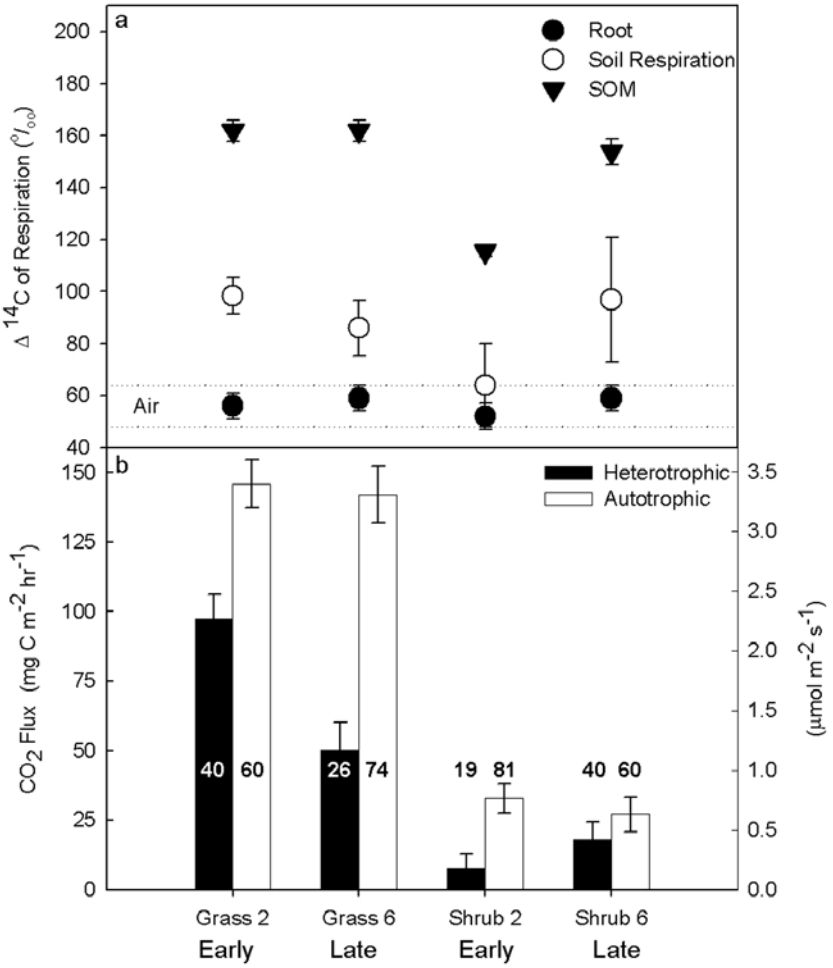

Figure 5. (a) Radiocarbon values for atmospheric air (dashed lines), root respiration (black circles), soil respiration (white circles), and SOM respiration (black downward triangles). Error bars represent ±1 standard deviation. (b) Soil respiration partitioning (isotope sampling time period mean flux) from heterotrophic (black) and autotrophic (white) sources. Numbers represent the percent of the total flux (100%) coming from that source. Error bars represent ±1 standard error.

of carbon fixed since 1963 ("bomb" ^{14}C) in both the grass (surface soil: 162 ± 4‰) and the shrub (surface soil: 115 ± 2‰, deep soil: 154 ± 5‰) ecosystems. Seasonal patterns in soil respiration $\Delta^{14}C$ signatures showed different trends between the two ecosystems. The grass soil respiration ^{14}C content decreased (98 ± 7 to 86 ± 10‰) and the shrub increased (64 ± 16 to 97 ± 24‰) from early to late growing season, respectively. Shrub soil respiration $\Delta^{14}C$ signatures exhibited much greater spatial variability, presumably due to more heterogeneous vegetation cover compared to the grass site.

4.5. Partitioning Soil Respiration Sources

[30] Partitioning soil respiration among heterotrophic and autotrophic sources resulted in noticeable differences between ecosystems, and the early and late growing season. Figure 5 shows the mean flux of CO_2 by each source during the isotope measurement period (8:00–14:00 h). Autotrophic sources (including rhizosphere respiration) accounted for 60% (early) to 74% (late) of total soil respiration in the grass, and 81% (early) to 60% (late) in the shrub ecosystem. The grass ecosystem, characterized by greater fluxes overall, had similar autotrophic component fluxes, 146 ± 9 and 142 ± 10 mg C m^{-2} h^{-1} in the early and late respectively, with a smaller contribution from the heterotrophic component in the late growing season (97 ± 9 and 49 ± 10 mg C m^{-2} h^{-1} early and late respectively). The shrub ecosystem, with smaller gross CO_2 fluxes overall, had a small decline in autotrophic fluxes between the early and late growing (33 ± 5 and 26 ± 6 mg C m^{-2} h^{-1} early and late respectively). However, unlike the grass ecosystem, heterotrophic contributions markedly increased (8 ± 5 and 18 ± 6 mg C m^{-2} h^{-1} early and late respectively). In the shrub ecosystem, this coincided with much higher concentrations of soil pore space CO_2 at 100 cm depth (~10,000 ppm versus ~3100 ppm) and a larger concentration gradient from depth to surface, in late growing season versus early growing season, respectively.

5. Discussion

5.1. The Magnitude of Soil Respiration

[31] Large differences were observed between soil respiration from the two vegetation communities, perennial

grasses and shrubs in the Owens Valley, CA. Most apparent was the magnitude of soil respiration, about 7 times greater in the grass ecosystem. The soil respiration rates measured in the grass ecosystem were at the upper end of previously reported soil respiration values from any ecosystem, and those from the shrub ecosystem at the lower end, similar to other desert ecosystem studies [*Raich and Schlesinger*, 1992; *Raich and Tufekcioglu*, 2000]. These two ecosystems were only several kilometers apart and experienced similar temperature and precipitation patterns, so why did soil respiration rates differ so greatly? We suggest physical differences in soil water availability and biological differences in plant allocation patterns and productivity were the major factors affecting the magnitude of both autotrophic and heterotrophic respiration sources.

[32] Soil moisture in the grass ecosystem was substantially greater for the entire period of measurements due to a higher water table, thus surface soil water-limitation was greater in the shrub ecosystem. The soil respiration rates stimulated by small precipitation events were short-lived and only minor contributors to growing season totals. This result was unlike other semi-arid ecosystem studies, which found dry season precipitation pulses to contribute significantly to soil respiration [*Huxman et al.*, 2004; *Xu and Baldocchi*, 2004; *Xu et al.*, 2004; *Misson et al.*, 2006]. Although, we believe that this result was more due to the small amount of rain observed and not necessarily the inherent response of the ecosystem. The precipitation contribution to annual soil respiration could be much greater than observed, as ~75% of annual precipitation occurred outside of the growing season (mostly in the form of snow) when measurements were lacking. The grass productivity belowground was intrinsically greater than that of the shrubs, producing both more autotrophic sources in growth and maintenance respiration and more heterotrophic substrates in fine root inputs available for microbial decomposition [*Janssens et al.*, 2001]. The large discrepancy in soil C content was also likely the result of plant productivity differences. These plant functional type differences were also demonstrated in a concurrent pulse-chase isotope labeling study reported by *Carbone and Trumbore* [2007], which showed 3 times greater allocation of new assimilates to respiration below- versus aboveground in the grasses compared to the shrubs. Other potential site differences that could not be evaluated were site history and land use. These factors were unlikely major contributors to soil respiration rates, because the isotopic analyses demonstrated the dominance of respired C fixed in recent decades when there were no land management changes.

5.2. Controls on the Seasonal Pattern of Soil Respiration

[33] On the seasonal timescale, temperature and soil moisture collectively explained most of the variability in soil respiration in both ecosystems, similar to analyses from other ecosystems [*Irvine and Law*, 2002; *Savage and Davidson*, 2003; *Reichstein et al.*, 2003]. At a coarse-resolution, the seasonal models adequately described the growing season variation in soil respiration by using a fixed basal respiration rate and temperature sensitivity, and parabolic soil moisture function. These simple temperature and moisture relationships undoubtedly integrated and masked phenological controls on soil respiration rates [*Curiel-Yuste et al.*, 2004]. Moreover, the higher-resolution measurements clearly established that in order to capture the dynamics of the diel form in soil respiration, both basal respiration and temperature sensitivity parameters must change with time, and the use of fixed model parameters for both ecosystems would result in biased estimates of soil respiration over seasonal timescales [*Richardson et al.*, 2006]. Additionally, these measurements demonstrated that shifts in the diel form occurred from one day to the next, suggesting that physiological thresholds and/or sudden phenological changes need to be better understood. Thus model parameters based on continuous functions may not be appropriate to describe these soil respiration patterns.

5.3. Seasonal Sources of Soil Respiration

[34] Soil respiration was mostly derived from plant sources in both the grass and shrub ecosystems in the early growing season, corresponding with the greatest root growth in surface soil layers in these ecosystem types [*Caldwell et al.*, 1977]. The autotrophic flux in the late growing season declined slightly in both ecosystems, we believe due to soil water deficit in upper soil layers, and plant phenological changes in root biomass and belowground allocation of new photosynthetic products [*Carbone and Trumbore*, 2007]. The late growing season heterotrophic component in the grass ecosystem decreased more so than the autotrophic, again likely due to surface soil moisture limitation. The increase in the shrub ecosystem heterotrophic component in the late growing season coincided with large increases in the CO_2 production at depth, likely the result of a vertical shift in the location of microbial decomposition due to progressive downward warming and drying of the soil profile over the growing season. The heterotrophic components in both ecosystems may have been under-estimated, as our experimental approach lumps the fast turnover of root exudates and mycorrhizal respiration with ''autotrophic'' respiration sources.

5.4. The Diel Pattern of Soil Respiration

[35] Interestingly, the magnitude of soil respiration differed between the grass and shrub ecosystems, but the major controls were similar on the diel timescale. In the early growing season, temperature was an excellent predictor of soil respiration in both ecosystems. In the middle to late growing season, as surface soil moisture decreased, soil respiration was progressively more decoupled from temperature. This indicated considerable substrate limitation on both autotrophic (in the allocation of new photosynthetic products to roots) and surface heterotrophic (through the diffusion of solutes through microbial cell membranes) [*Skopp et al.*, 1990] sources. The result of decreasing soil moisture and its direct and indirect effects on substrate availability was also confirmed in the declining amplitude and temperature sensitivity of soil respiration over the growing season, shown by the mean diel cycle analyses and empirical models [*Reichstein et al.*, 2002]. The seasonal change observed in the temperature-flux relationships demonstrates additional controls on soil respiration other than surface soil and air temperature. Like observations in other ecosystems, we hypothesize that this could be photosynthesis [*Högberg et al.*, 2001; *Ekblad and Högberg*, 2001;

Bowling et al., 2002; *Tang et al.*, 2005; *Baldocchi et al.*, 2006; *Liu et al.*, 2006]. However, while most of these studies identified time lags of several hours to days between assimilation and soil respiration, our observations required a more rapid connection because rates peaked in the mid-morning before temperature.

[36] We have no diurnal leaf gas-exchange measurements at these sites to prove this tight link between assimilation and soil respiration. Yet, the parallel labeling study demonstrated the presence of new labeled assimilates in soil respiration in less than 4 h after assimilation. This transport was arguably much faster, as it was determined by the first sampling time point after labeling [*Carbone and Trumbore*, 2007]. This same study showed that autotrophic soil respiration was mostly derived from the current day's photosynthate produced in the upper 10 cm of the soil. Therefore it is reasonable, particularly in these short stature plants, with the initiation of photosynthesis and phloem loading in the early morning hours, that the translocation of new assimilates and/or the propagation of pressure and concentration fronts could produce the rapid substrate supply available for soil respiration [*Thompson and Holbrook*, 2004].

[37] The nuances in the shape of the diel cycle may provide additional insight into the photosynthetic controls on soil respiration. We hypothesize that the bimodal pattern of soil respiration observed in the middle and late growing season, with the consistent depression at mid-day, reflected plant physiological responses to water-stress. We can only speculate on the exact mechanism, but suggest that VPD and its influence on stomatal conductance and photosynthetic assimilation rates may have been the cause. This link between VPD and soil respiration has been reported before in forested ecosystems with longer time lags [*Ekblad and Högberg*, 2001; *Bowling et al.*, 2002; *Baldocchi et al.*, 2006].

[38] Under dry environmental conditions, both theoretical and experimental evidence have shown that in order to optimize carbon gain and water loss, many plants have bimodal diurnal assimilation patterns due to partial stomatal closure [*Cowan*, 1977; *Schulze and Hall*, 1982; *Brodribb and Holbrook*, 2004]. Along these same lines, in the late growing season, the diel peak in soil respiration occurred in the morning hours, when shrubs were photosyntheically active [Pataki, personal communication] and VPD was at a minimum. As VPD increased during the day, soil respiration rates dropped. This seasonal change in the pattern of diurnal leaf gas-exchange has been observed before in these shrubs species in the Owens Valley and other Great Basin ecosystems [*Donovan et al.*, 1996; *Caldwell et al.*, 1977]. In the grass ecosystem, leaf gas-exchange would have been likely less affected by water-stress and high temperatures due to the dominance of plants with the C_4 photosynthetic pathway [*Schulze and Hall*, 1982]. Thus a bimodal shape of assimilation could be sustained through the late summer in the grasses, and be reflected in the bimodal shape of soil respiration.

[39] Other explanations for these diel patterns could be dynamical or heterotrophic in nature. One hypothesis we investigated to explain the mid-morning rise in soil respiration was heterotrophic activity stimulated by increased water availability occurring overnight. Water increases could be driven by condensation (or just absorption of water) on soil and litter surfaces when temperatures approach the dew point, or from hydraulic lift by surface roots. The use and exhaustion of this water source could explain the initial peak in the bimodal pattern of soil respiration, while temperature and autotrophic activity (driven by PAR) may explain the latter peak. Yet, we found no evidence of condensation occurring at the sites, and soil surface relative humidity probes never reached saturation during the entire measurement period (excluding small rain events). Hydraulic lift has been observed in *Sarcobatus vermiculatus* before [*Donovan et al.*, 1996], but the diel change in surface soil water content measured by our sensors was very small, and remained at matric potentials (<-1500 kPa) that inhibit microbial respiration [*Skopp et al.*, 1990]. However, we cannot rule out this hypothesis or other physical processes such as soil pore space "venting" [*Hirsch et al.*, 2004] and slower time-lagged diffusion processes like that described by *Stoy et al.* [2007] or *Riveros-Iregui et al.* [2007] which also could have contributed to these unique patterns.

5.5. Linking the Diel Cycle With Plant and Microbial Sources

[40] The overlap between radiocarbon source partitioning and diel measurements of soil respiration allowed us to look in more detail at the controls and sources of soil respiration at two time points (early and late growing season). In the early growing season, the excellent correlation of shrub soil respiration with air temperature likely reflected plant sources driving respiration rates. The grass ecosystem soil respiration correlation with 2 cm soil temperature demonstrated the more balanced contribution from the surface microbial component. In the late growing season, the shrub soil respiration had decreased and decoupled temperature sensitivity, and an elevated basal rate. This correlated with smaller plant contributions (primarily occurring in the mid-morning, we believe driven by photosynthetic activity) and enhanced microbial decomposition deep in the soil profile (which experienced much smaller diel temperature fluctuations that were temporally out of phase with the surface temperature). In the grass ecosystem, the temporal disconnect of temperature and flux, and the lower basal respiration rate coincided with the dominance of contributions from plant sources.

[41] These results suggest that autotrophic component is likely more dynamic over the diel time period due to both the influence of photosynthesis and the greater temperature sensitivity of autotrophic respiration [*Boone et al.*, 1998]. The heterotrophic component is likely less dynamic, particularly when surface soil moisture is limiting, and maybe better observed in slower changes in the basal respiration rate. Yet, it is simplistic to assume that autotrophic sources are responsible for all of the amplitude of the diel cycle, and heterotrophic sources determine the basal respiration rate, and our measurements disprove this assumption in the time periods where the isotopes were sampled. For example, phenological changes in root biomass will influence the basal respiration rate, and heterotrophic sources will be sensitive to diel temperature changes, and thus must contribute to the amplitude.

[42] It is important to mention that the isotopic measurements integrated soil respiration between 8:00 and 14:00 h, and the partitioning may be biased toward sources contrib-

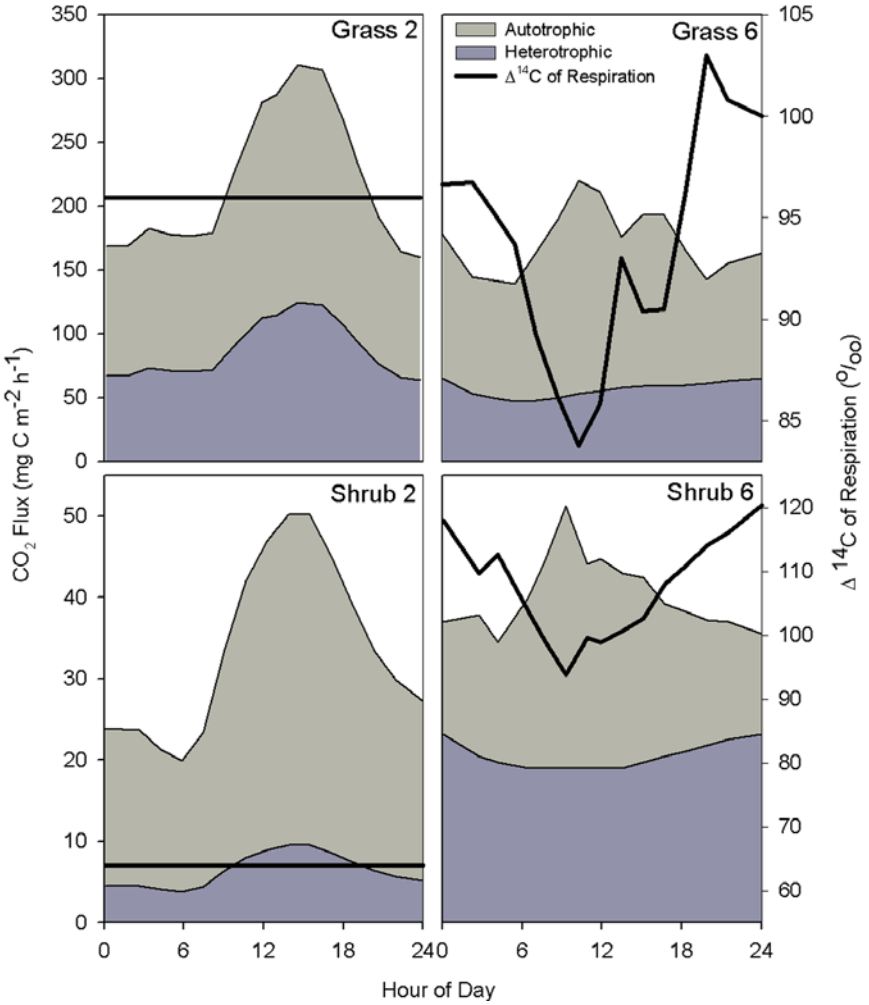

Figure 6. Hypothetical autotrophic (grey shaded) and heterotrophic (dark grey shaded) contributions to the diel course of soil respiration in mg C m^{-2} h^{-1} (left *y* axis), and expected $\Delta^{14}C$ signature of soil respiration (black line) in per mil (‰, right *y* axis) in the grass and shrub ecosystems during the early (period 2) and late (period 6) growing season.

uting to soil respiration during these hours of the day. If photosynthesis was driving autotrophic sources in the late growing season preferentially in the mid-morning, then the $\Delta^{14}C$ signatures of soil respiration reflected this. In Figure 6, we hypothetically show how the $\Delta^{14}C$ of soil respiration would have been affected if the fluxes from autotrophic and heterotrophic sources changed over the mean diel cycle in the shrub ecosystem. In the early growing season, we hypothesized that both autotrophic and heterotrophic sources were in phase and driven by temperature, and therefore the $\Delta^{14}C$ signature of soil respiration would remain the same over the course of the diel cycle, and sampling at anytime of day would be representative. In the late growing season, we hypothesized that autotrophic sources were morning-skewed due to constraints on photosynthetic activity. Heterotrophic sources were emanating from deeper in the soil profile due to surface water limitation, and thus more constant over the diel cycle. This results in a ~20–25‰ range in $\Delta^{14}C$ signature of soil respiration over the diel cycle. Also, consequently, 8 and 11% lower autotrophic contribution over 24 h versus the time period we sampled in both grass and shrub ecosystems respectively. For these reasons, we recommend that future isotope partitioning studies collect samples that integrate 24 h of soil respiration, or even better, multiple samples over the course of 24 h. We note that with any soil respiration partitioning technique (i.e., isotope, trenching, girdling, and spatial separation), a daytime sample of will have different source biases dependent on ecosystem function. If we had the foresight in this study, more careful isotope samples would have allowed us to quantitatively assess the diel contributions of autotrophic and heterotrophic sources, and how this determines the diel course of soil respiration.

[43] Interestingly, even if the timing of sampling led us to overestimate autotrophic contributions in the late growing season, total autotrophic contributions were either equivalent or greater in both ecosystems when no hysteresis was observed in the temperature-flux relationship. This implies that presence of these non-linearities between temperature and respiration did not necessarily infer greater contribution of plant sources. As water became more limiting, aboveground plant physiological responses to water-stress may

have been increasingly important controls on the diel shape. Thus we hypothesize that the different temperature-flux relationships observed over the diel cycle were the result of this strong photosynthetic influence on the timing of soil respiration rates, not merely the partitioning of its sources. Microbial decomposition was likely less responsible for the amplitude and shape of the diel cycle, particularly in the late growing season when surface moisture was depleted. Nonetheless, this study has demonstrated that the extent to which such processes contribute to soil respiration on the diel timescale could be quantified with more strategic isotope sampling.

6. Conclusions and Implications

[44] Our results have important implications for constructing mechanistic models of soil respiration that can scale across ecosystems and in time. We demonstrated that vegetation type played an important role in the magnitude and seasonality of soil respiration. Basal soil respiration rates reflected vegetation productivity and phenology, and the seasonal changes in temperature and moisture. These controls are likely ecosystem dependent and difficult to model without prior knowledge of ecosystem specific plant allocation patterns. In these particular ecosystems a shift in vegetation type from grasses to shrubs would likely alter soil respiration rates significantly due to inherent differences in plant allocation patterns to new biomass structures, growth and maintenance respiration, and the partitioning of this allocation above- versus below-ground.

[45] The diel course of soil respiration was largely determined by autotrophic activity in these ecosystems. Photosynthesis and leaf physiology may have played an important role in substrate supply to root respiration on diel timescales. Hypothesized relationships with VPD and sudden changes in the structure of the diel pattern of soil respiration would not have been identified without the high-resolution automated measurements. However, simultaneous photosynthesis and soil respiration measurements would be required to prove the rapid link. Surprisingly, these desert ecosystems appear to be good systems to investigate such relationships, and the information gathered from them could provide insight into other ecosystems where diel signals are not as clearly defined. Furthermore, radiocarbon isotope samples taken throughout the growing season and over diel cycles provide powerful tests of hypotheses about the causes of changing soil respiration patterns. For these reasons, we suggest that a mechanistic understanding of soil respiration requires that future studies incorporate isotope partitioning with automated measurements of soil respiration, aboveground physiology, below-ground phenology, and allocation studies in order to better quantify these vegetation controls on soil respiration rates and sources.

[46] **Acknowledgments.** We thank Xiaomei Xu for laboratory assistance and ^{14}C expertise. Field work and technical assistance was provided by Claudia Czimczik, Andrew Delaney, Chris Doughty, Aaron Fellows, Matt Khosh, Kelsey McDuffee, Thien Nyguen, Cameron Porter, Ed Read, Sami Rifai, Adrian Rocha, Imran Sheikh. Robert Harrington and Aaron Steinwand at Inyo County Water Department provided additional field site information. The Los Angeles Department of Water and Power provided access to field sites. Michael Goulden and two anonymous reviewers provided comments that improved the quality of this manuscript. This work was supported by The Kearney Foundation of Soil Science.

References

Asner, G. P., S. Archer, R. F. Hughes, R. T. Ansley, and C. A. Wessman (2003), Net changes in regional woody vegetation cover and carbon storage in Texas Drylands, 1937–1999, *Global Change Biol.*, *9*, 316–335.

Baldocchi, D., J. W. Tang, and L. K. Xu (2006), How switches and lags in biophysical regulators affect spatial-temporal variation of soil respiration in an oak-grass savanna, *J. Geophys. Res.*, *111*, G02008, doi:10.1029/2005JG000063.

Boone, R. D., K. J. Nadelhoffer, J. D. Canary, and J. P. Kaye (1998), Roots exert a strong influence on the temperature sensitivity of soil respiration, *Nature*, *396*, 570–572.

Bowling, D. R., N. G. McDowell, B. J. Bond, B. E. Law, and J. R. Ehleringer (2002), C-13 content of ecosystem respiration is linked to precipitation and vapor pressure deficit, *Oecologia*, *131*, 113–124.

Brodribb, T. J., and N. M. Holbrook (2004), Diurnal depression of leaf hydraulic conductance in a tropical tree species, *Plant Cell Environ.*, *27*, 820–827.

Caldwell, M. M., R. S. White, R. T. Moore, and L. B. Camp (1977), Carbon balance, productivity, and water-use of cold-winter desert shrub communities dominated by C_3 and C_4 species, *Oecologia*, *29*, 275–300.

Carbone, M. S., and S. E. Trumbore (2007), Contribution of new assimilates to respiration by perennial grasses and shrubs: Allocation patterns and residence times, *New Phytol.*, *176*, 124–135.

Carbone, M. S., and R. Vargas (2008), Automated soil respiration measurements: New challenges, information, and opportunities, *New Phytol.*, *177*, 295–297.

Cowan, I. R. (1977), Stomatal behaviour and environment, *Adv. Bot. Res.*, *4*, 117–228.

Cox, P. M., R. A. Betts, C. D. Jones, S. A. Spall, and I. J. Totterdell (2000), Acceleration of global warming due to carbon-cycle feedbacks in a coupled climate model, *Nature*, *408*, 184–187.

Craine, J. M., D. A. Wedin, and F. S. Chapin (1999), Predominance of ecophysiological controls on soil CO_2 flux in a Minnesota grassland, *Plant Soil*, *207*, 77–86.

Curiel-Yuste, J., I. A. Janssens, A. Carrara, and R. Ceulemans (2004), Annual Q(10) of soil respiration reflects plant phenological patterns as well as temperature sensitivity, *Global Change Biol.*, *10*, 161–169.

Czimczik, C. I., S. E. Trumbore, M. S. Carbone, and G. C. Winston (2006), Changing sources of soil respiration with time since fire in a boreal forest, *Global Change Biol.*, *12*, 957–971.

Davidson, E. A., E. Belk, and R. D. Boone (1998), Soil water content and temperature as independent or confounded factors controlling soil respiration in a temperate mixed hardwood forest, *Global Change Biol.*, *4*, 217–227.

Davidson, E. A., I. A. Janssens, and Y. Q. Luo (2006), On the variability of respiration in terrestrial ecosystems: moving beyond Q10, *Global Change Biol.*, *12*, 154–164.

Donovan, L. A., J. H. Richards, and M. W. Muller (1996), Water relations and leaf chemistry of Chrysothamnus nauseosus ssp Consimilis (Asteraceae) and Sarcobatus vermiculatus (Chenopodiaceae), *Am. J. Bot.*, *83*, 1637–1646.

Ekblad, A., and P. Högberg (2001), Natural abundance of C-13 in CO_2 respired from forest soils reveals speed of link between tree photosynthesis and root respiration, *Oecologia*, *127*, 305–308.

Elmore, A. J., J. F. Mustard, and S. J. Manning (2003), Regional patterns of plant community response to changes in water: Owens Valley, California, *Ecol. Appl.*, *13*, 443–460.

Gaudinski, J. B., S. E. Trumbore, E. A. Davidson, and S. H. Zheng (2000), Soil carbon cycling in a temperate forest: Radiocarbon-based estimates of residence times, sequestration rates and partitioning of fluxes, *Biogeochemistry*, *51*, 33–69.

Goulden, M. L., and P. M. Crill (1997), Automated measurements of CO_2 exchange at the moss surface of a black spruce forest, *Tree Physiol.*, *17*, 537–542.

Hanson, P. J., N. T. Edwards, C. T. Garten, and J. A. Andrews (2000), Separating root and soil microbial contributions to soil respiration: A review of methods and observations, *Biogeochemistry*, *48*, 115–146.

Hirsch, A. I., S. E. Trumbore, and M. L. Goulden (2004), The surface CO_2 gradient and pore-space storage flux in a high-porosity litter layer, *Tellus Ser. B-Chem. Phys. Meteorol.*, *56*, 312–321.

Högberg, P., A. Nordgren, N. Buchmann, A. F. S. Taylor, A. Ekblad, M. N. Högberg, G. Nyberg, M. Ohoson-Löfvenius, and D. J. Read (2001), Large-scale forest girdling shows that current photosynthesis drives soil respiration, *Nature*, *411*, 79–789.

Hollett, K. J., W. R. Danskin, W. F. McCaffrey, and C. L. Walti (1991), Geology and water resources of Owens Valley, California, *U.S. Geol. Surv. Water Supply Pap.*, *2370-B*.

Huxman, T. E., K. A. Snyder, D. Tissue, A. J. Leffler, K. Ogle, W. T. Pockman, D. R. Sandquist, D. L. Potts, and S. Schwinning (2004), Precipitation pulses and carbon fluxes in semiarid and arid ecosystems, *Oecologia*, *141*, 254–268.

Irvine, J., and B. E. Law (2002), Contrasting soil respiration in young and old-growth ponderosa pine forests, *Global Change Biol.*, *8*, 1183–1194.

Jackson, R. B., et al. (2000), Belowground consequences of vegetation change and their treatment in models, *Ecol. Appl.*, *10*, 470–483.

Janssens, I. A., et al. (2001), Productivity overshadows temperature in determining soil and ecosystem respiration across European forests, *Global Change Biol.*, *7*, 269–278.

King, J. A., and R. Harrison (2002), Measuring soil respiration in the field: An automated closed chamber system compared with portable IRGA and alkali absorption methods, *Commun. Soil Sci. Plant Anal.*, *33*, 403–423.

Kuzyakov, Y., and W. Cheng (2001), Photosynthesis controls of rhizosphere respiration and organic matter decomposition, *Soil Biol. Biochem.*, *33*, 1915–1925.

Liu, Q., N. T. Edwards, W. M. Post, L. Gu, J. Ledford, and S. Lenhart (2006), Temperature-independent diel variation in soil respiration observed from a temperate deciduous forest, *Global Change Biol.*, *12*, 2136–2145.

Misson, L., A. Gershenson, J. W. Tang, M. McKay, W. X. Cheng, and A. Goldstein (2006), Influences of canopy photosynthesis and summer rain pulses on root dynamics and soil respiration in a young ponderosa pine forest, *Tree Physiol.*, *26*, 833–844.

Pataki, D. E., S. A. Billings, E. Naumburg, and C. Goedhart (2008), Water sources and nitrogen relations of grasses and shrubs in phreatophytic communities of the Great Basin Desert, *J. Arid Environ.*, in press.

Phillips, D. L., and J. W. Gregg (2001), Uncertainty in source partitioning using stable isotopes, *Oecologia*, *127*, 171–179.

Raich, J. W., and C. S. Potter (1995), Global patterns of carbon-dioxide emissions from soils, *Global Biogeochem. Cycles*, *9*(1), 23–36.

Raich, J. W., and W. H. Schlesinger (1992), The global carbon-dioxide flux in soil respiration and its relationship to vegetation and climate, *Tellus, Ser. B-Chem. Phys. Meteorol.*, *44*, 81–99.

Raich, J. W., and A. Tufekcioglu (2000), Vegetation and soil respiration: Correlations and controls, *Biogeochemistry*, *48*, 71–90.

Raich, J. W., C. S. Potter, and D. Bhagawati (2002), Interannual variability in global soil respiration, 1980–94, *Global Change Biol.*, *8*, 800–812.

Reichstein, M., J. D. Tenhunen, O. Roupsard, J. M. Ourcival, S. Rambal, S. Dore, and R. Valentini (2002), Ecosystem respiration in two Mediterranean evergreen Holm Oak forests: Drought effects and decomposition dynamics, *Functional Ecol.*, *16*, 27–39.

Reichstein, M., et al. (2003), Modeling temporal and large-scale spatial variability of soil respiration from soil water availability, temperature and vegetation productivity indices, *Global Biogeochem. Cycles*, *17*(4), 1104, doi:10.1029/2003GB002035.

Richardson, A. D., et al. (2006), Comparing simple respiration models for eddy flux and dynamic chamber data, *Agric. For. Meteorol.*, *141*, 219–234.

Riveros-Iregui, D. A., R. E. Emanuel, D. J. Muth, B. L. McGlynn, H. E. Epstein, D. L. Welsch, V. J. Pacific, and J. M. Wraith (2007), Diurnal hysteresis between soil CO_2 and soil temperature is controlled by soil water content, *Geophys. Res. Lett.*, *34*, L17404, doi:10.1029/2007GL030938.

Savage, K. E., and E. A. Davidson (2003), A comparison of manual and automated systems for soil CO_2 flux measurements: Trade-offs between spatial and temporal resolution, *J. Exp. Bot.*, *54*, 891–899.

Saxton, K. E., W. J. Rawls, J. S. Romberger, and R. I. Papendick (1986), Estimating generalized soil-water characteristics from texture, *Soil Sci. Soc. Am. J.*, *50*, 1031–1036.

Schlesinger, W. H., J. F. Reynolds, and G. L. Cunningham (1990), Biological feedbacks in global desertification, *Science*, *247*, 1043–1048.

Schulze, E. D., and A. E. Hall (1982), Stomatal responses, waterloss and CO_2 assimilation rates of plants in contrasting environments, in *Encyclopedia of Plant Physiology*, vol. 12B, *Physiological Plant Ecology II: Water Relations and Carbon Assimilation*, edited by O. L. Lange et al., pp. 181–230, Springer-Verlag, Germany.

Schuur, E. A., and S. E. Trumbore (2006), Partitioning sources of soil respiration in boreal black spruce forest using radiocarbon, *Global Change Biol.*, *12*, 165–176.

Skopp, J., M. D. Jawson, and J. W. Doran (1990), Steady-state aerobic microbial activity as a function of soil-water content, *Soil Sci. Soc. Am. J.*, *54*, 1619–1625.

Southon, J., G. Santos, K. Druffel-Rodriguez, E. Druffel, S. Trumbore, X. Xu, S. Griffin, S. Ali, and M. Mazon (2004), The Keck Carbon Cycle AMS laboratory, University of California, Irvine: Initial operation and a background surprise, *Radiocarbon*, *46*, 41–49.

Stoy, P. C., S. Palmroth, A. C. Oishi, M. B. S. Siqueira, J. Y. Juang, K. A. Novick, E. J. Ward, G. G. Katul, and R. Oren (2007), Are ecosystem carbon inputs and outputs coupled at short time scales? A case study from adjacent pine and hardwood forests using impulse-response analysis, *Plant Cell Environ.*, *30*, 700–710.

Stuiver, M., and H. A. Polach (1977), Reporting of C-14 data - Discussion, *Radiocarbon*, *19*, 355–363.

Subke, J. A., I. Inglima, and M. F. Cotrufo (2006), Trends and methodological impacts in soil CO_2 efflux partitioning: A metaanalytical review, *Global Change Biol.*, *12*, 921–943.

Tang, J. W., and D. D. Baldocchi (2005), Spatial-temporal variation in soil respiration in an oak-grass savanna ecosystem in California and its partitioning into autotrophic and heterotrophic components, *Biogeochemistry*, *73*, 183–207.

Tang, J. W., D. D. Baldocchi, and L. Xu (2005), Tree photosynthesis modulates soil respiration on a diurnal time scale, *Global Change Biol.*, *11*, 1298–1304.

Thompson, M. V., and N. M. Holbrook (2004), Scaling phloem transport: Information transmission, *Plant Cell Environ.*, *27*, 509–519.

Trumbore, S. (2006), Carbon respired by terrestrial ecosystems - Recent progress and challenges, *Global Change Biol.*, *12*, 141–153.

Xu, L. K., and D. D. Baldocchi (2004), Seasonal variation in carbon dioxide exchange over a Mediterranean annual grassland in California, *Agric. For. Meteorol.*, *123*, 79–96.

Xu, L. K., D. D. Baldocchi, and J. W. Tang (2004), How soil moisture, rain pulses, and growth alter the response of ecosystem respiration to temperature, *Global Biogeochem. Cycles*, *18*, GB4002, doi:10.1029/2004GB002281.

Xu, X., S. E. Trumbore, and S. Zheng (2007), Modifying a sealed tube zinc reduction method for preparation of AMS graphite targets: Reducing background and attaining high precision, *Nucl. Instrum. Methods Phys. Res., Section B259*, 320–329.

M. S. Carbone, Department of Geography, University of California, 1832 Ellison Hall, Santa Barbara, CA 93106-4060, USA. (mcarbone@icess.ucsb.edu)

S. E. Trumbore and G. C. Winston, Department of Earth System Science, University of California, 3200 Croul Hall, Irvine, CA 92697-3100, USA.